Journal of Polymer Science and Engineering (2018) Volume 1
doi:10.24294/jpse.v1i4.1048

Original Research Article

On Some Key Problems of Modern Polymer Rheology

Igor MACKAROV

Bogdanovich st. 55/232, Minsk, 220123, Belarus, E-mail: Mackarov@gmx.net

ABSTRACT

Control of key technological and benchmark flows of polymer fluids poses many challenges. Some of them are nowadays under active investigation and rather far from a complete understanding. This review considers such phenomena as both practically important and governed by fundamental laws of rheology and non-linear fluid mechanics. We observe shear bands in polymeric and other complex structured fluids (like wormlike micellar solutions or soft glassy materials), birefrigerent strands, peculiarities of stress and pressure losses in fluids moving through complex shape domains. These and other processes involve inhomogeneity, instabilities and transient modes in creeping flows. In practical aspect, this is of interest in such industrial process as polymer flooding for Enhanced Oil Recovery (EOR), where a flow inhomogeneity affects a polymer solution injectivity and residual oil saturation. The value of viscoelasticity in the polymer flooding is estimated. The observation is concluded through some new results on relation between polymer concentration in solutions and viscoelastic traits of benchmark flows.

***Keywords*:** Shear Banding; Birefrigerent Strands; Pressure Losses; Polymer Injectivity; Benchmark Flows

1. Introduction

The aim of this work is to look into some specific viscoelastic phenomena of polymer fluids that can affect control of flows. We are going to feature them as both practically important and governed by common fundamental laws of rheology and non-linear fluid mechanics. It is important to emphasize that a great many complex traits of non-Newtonian flows are not independent. As suggested by[1], "*viscoelasticity, yielding, flow instabilities and turbulence, flow-induced structures, shear banding* and other types of shear localization, all these phenomena and more show us various aspects of a common fate". Add to this list *quasi-periodic regimes of viscoelastic flows, flows reversals*[2,3,4], and *bifurcations in stationary points of flows resulting from the flow vorticity accumulation in these points*[4,5]. We are going to analyze some of these features and their interconnections in experimental and industrial conditions. In addition, some other representatives of the soft matter - that are partly overlapped with polymeric materials - will be considered. Such materials as *wormlike micellar surfactant solutions or soft glassy materials* undergo close dynamic processes and reveal similar behavior.

The first section concerns the feature that is itself a combination of a number of specific phenomena.

2. Share banding

We consider here formation of share bands, *viz*., the zones where the fluid undergoes extremely high strains, which considerably affects the flow structure and properties. This phenomenon has been long ago identified by specialists in geology and oil production.

Review[1] presents share banding as a sophisticated subject composed of a set of specific nonlinear phenomena. They are usually connected in a nontrivial way so that it is not easy to isolate the cause from the effect in such connections. Herein, these nonlinear traits are usually so fundamental that they often predetermine similar behavior of *polymeric* and *soft glassy* materials.

The polymeric fluids are often studied in terms of *continuous media mechanics* treating soft matter as sitting in between the ideal Hookean elastic solid, and the ideal Newtonian viscous fluid. The mechanical approach, however, is not self-sustained with respect to such fluids as wormlike micellar surfactant solutions, polymer solutions, star polymers, emulsions, and the list goes on. They often have "mesoscopic" constituents with

doi: 10.24294/jpse.v1i4.1048

the length scale ranging between the molecular and the flow scales. This combination of mechanical and structural traits is admitted to be the reason of shear banding phenomena. They are studied by direct experimental observations and theoretically by means of tube models, as well as specific mechanical models with empiric information. Such information, in particular, can have a form of diffusive terms accounting for non-equilibrium transient microscopic restructuring processes, for example, at the interface between the shear bands[1,6]. Such are *the diffusive Johnson-Segalman model (d-JS) or the diffusive Giesekus model (d-Giesekus)*. A compromise between microscopic and continuum levels is *the Rolie–Poly model*. It incorporates convected constraint release (CCR)[7] and tube stretching. These models are able to successfully predict *a nonmonotonic constitutive curve*, admittedly one of the principal factors leading to shear banding[1,6,8,9].

The phenomenon is often a rich source of elastic instabilities, like any flow feature involving large strains[3]. It can provide rather specific forms of instability, for example, jetting behavior of flows in rectangular channels[10]. The principal hitherto observed features of the instabilities induced by gradient and vorticity bandings are: significant role of the normal stresses gap across the bands interface, important value of coupling to concentration of the fluid constituents, the possibility of "narrowly localized but still unsteady interfaces"[11].

Note the results of work[12] considering instability of the Johnson-Segalman fluid involved in the Couette flow with share banding. The profiles of the velocity perturbations depicted in this work's **Figure 5** look surprisingly similar to the distributions of velocity of the accelerating Couette *Upper Convected Maxwell* flow presented in **Figure 7** of[13] even though these two flows stay far apart. This is likely to point to ubiquitous character of basic viscoelastic phenomena (concurrency between the elastic factor and the dissipation of the mechanical movement energy).

The soft glassy materials (SGM) involve "a distribution of mesoscopic fluid elements that hop from trap to trap at a rate which is enhanced by the work done to strain the fluid element"[14]. From this perspective, shear banding is therefore treated as a flow-induced transition of fluid elements *(i)*, or mutual effects of shear and attractive interactions between the fluid elements *(ii)*, or interaction between the flow and concentration of the fluid constituents *(iii),* The last point may show up in the form of fragmentation of an initially solid sample into blocks separated by fluidized regions. Other features of shear banding in flows of SGM are significant wall slip and sophisticated time-dependent flows restructuring. For example, the Couette flow can involve intermittent switching from plug-like flow to linear velocity profiles[15].

Typical soft glassy materials revealing complex heterogeneous flow behavior are *glassy colloidal star polymers and Laponite suspensions*. The latter are defined as "a synthetic clay of the hectorite type made of heavily charged disc-shaped particles of diameter 25–30 nm, thickness 1 nm, and density 2.5 $g \cdot cm^{-3}$ "[15].

3. Birefrigerent strands

Unlike shear bands – identified by high shear rate interfaces – birefrigerent strands are flow zones of anomalously high stresses located in the flow down the local zones of significant fluid strains[16]. Because of limited relaxation time in a viscoelastic fluid, such zones are often go far downstream from the sources of high strains (obstacles, stagnation points etc.). The contraction/expansion flows where this phenomenon is observed are encountered in a number of important physiological and industrial processes[17], "including porous media flow, which is relevant to Enhanced Oil Recovery"[18]. *Enhanced Oil Recovery* is covered in Section 4.

Birefrigerent strands in conjunction with microfluidic *oscillating stagnation flows* (cf. Section 5) are considered in paper[18]. In such flows multiple stagnation points along the stream are observed. The situation is close to conditions in porous media. It turns out that the lower a stagnation point down the flow, the more distinct the strand near it is (in terms of higher local viscosity and enhanced pressure drop). This is explained by the transfer of pre-stretched material from one stagnation point to another thus facilitating further stretching downstream.

The cross-slot experiments were performed with

0.03 wt. % solutions of *atactic polystyrene* (*aPS*) in *dioctyl phthalate* (*DOP*). As "DOP is a fairly viscous (η = 0.046 Pa·s) theta solvent for aPS at close to room temperature"[18], the mixture proved fairly viscous and elastic.

Mention the value of *finite polymer extensibility* in highly strained flows. As reported in work[19], it is supposed to be the reason of such specific phenomenon as *back switch from turbulent to laminar regime* in creeping highly elastic flows.

Apparently, account of limited extensibility is also important in *theoretical and numerical studies*. For this, in particular, the *Finitely Extensible Nonlinear Elastic* (*FENE*) *model* is highly applicable nowadays to the flows with birefrigerent strands.

One more point of computational studies is failures to reach convergence of numerical solutions in high deformation zones. This sometimes results from improper omission of convective terms in rheological models and the momentum equation when a highly elastic fluid flow is considered "inertialess". With respect to such structural elements as birefrigerent strands, convective terms may be of order of other terms because, however slow a flow is, the space derivatives of velocities are high enough in the relevant zones. This point is discussed in much detail in[4,20,21].

4. Pressure losses of flows in complex domains

Choice of a correct value of the pressure is often crucial in situations of complex flows. Correct pressure is necessary to ensure an optimal chemical regime of polymerization[22]. High flow rates of polymer melts in dies and molds sometimes require pressure as high as 100 MPa[23]. It is natural to seek opportunities of escaping exceptional costs on setting too high pressure. In this, the pressure needed for optimal organization of the flow significantly depends in many cases on viscous and elastic forces inside a flow. This dependency is thus an important research subject.

Such is the case of viscoelastic flows in **capillaries**. As per paper[24], however simple capillaries' geometry is, it poses rather complicated problems in setting/determination of pressure inlet-outlet losses. Due to small cross-section area, high strains are developed in the flow. This invokes significant viscoelastic features so that the shear stresses and the pressure needed to compensate them depend upon the relation between the period of the flow restructuring and the polymer relaxation time. According to the authors of the cited paper, correct choice of the pressure requires construction of a universal dependency between pressure losses and the fluid macrostructures relaxation time. In this, consideration of *continuous spectrum* of the relaxation times is needed[25] based on thorough measurements and precise and sophisticated mathematical models.

A very different example of viscoelasticity manifestation in dynamic conditions is motion of water in topologically complex domains. Such are branched **Y-shaped pipelines** made of *high density polyethylene* (*HDPE*) and conducting water[26,27]. Action of *water hammers* can bring about pressure waves whose behavior evidently requires strict control. Under the highly changeable pressure, the material of a tube turns out to reveal viscoelastic behavior. Account of viscoelasticity makes it possible to determine very refined patterns of flows propagation and reflection to ensure pressure control in practice.

5. Flooding in oil industry

The above considered point of pressure losses play a significant economic role in oil production: "the energy required to transport heavy viscous crude oil in long pipes can be considerably reduced by the addition of small amounts of water to the crude resulting in reduced pumping costs"[28].

Another way to diminish pressure losses is to reduce the oil viscosity by addition of surfactant and stabilizing polymer components. Significant results on diminishing viscosity of heavy oils by this way are reported in[29].

Enhanced Oil Recovery (*EOR*) is a regular effective technique in oil industry. It aims at increase of the amount of crude oil that can be extracted from an oil field. Present some conclusions of survey[30] that provides comparative analyses of EOR based on *water* and *polymer* flooding. One of the main points of this work is as follows: "Because it has a higher success rate, polymer flooding is the most commonly applied

chemical EOR technique". This survey suggests that it is *viscoelasticity* that plays significant role in EOR with polymer flooding. This is confirmed by[31].

Four mechanisms to reduce residual oil saturation specific for a viscoelastic polymer solution have been identified. They are:

1. the pulling mechanism,
2. the stripping mechanism,
3. the mechanism of the oil-thread flow,
4. the mechanism of the shear-thickening effect.

Consider in more detail the third and fourth mechanisms as being the most specific for viscoelastic mixtures.

The third mechanism consists in formation of down-flowing oil threads out of the residual oil and onset of oil banks as a result of their interaction with the oil flowing up. The normal force of viscoelastic polymer solution "helps the oil thread to maintain its uniform cylindrical shape that prevents breakage"[30].

The fourth mechanism, the most crucial, is due to significantly elongational or extensional nature of a polymer solution flow past the structures of a porous medium yielding high shear rates. According to the survey, if the polymer is viscoelastic *the apparent viscosity is increased* (dilatant behavior). Experiments with polyacrylamide detected this behavior in porous materials, while it was not observed in rheometric flows at comparable shear rates

Likewise, in industrial polymer flooding apparent viscosity of a polymer solution is increased in *high-permeability zones*. The solution is therefore directed into *low-permeability zones* thus improving the sweep efficiency.

It is of interest to look into the reasons of the apparent viscosity increase and manifestation of viscoelasticity in general. In that regard, mention research[32], whose subject matter is a purely elastic instability of viscoelastic flows in complex small channels. An interesting mechanism of elastic energy accumulation has been observed there. The thing is that a streamline obviously follows the shape of the channel's boundary the more closely, the closer it is to the boundary. At the same time, the further the streamline from the boundary, the smoother it is, the less it "preserves the image of the boundary". Thus, the shapes of adjacent streamlines are different. When a macromolecule moves along such streamlines, it gets strained, for different parts of the molecule move differently. The elastic energy is thus accumulated. That not only brings about instability of the flow with small inertia, but also increases the apparent viscosity. This is because a strained macromolecule applies higher resistance to the flow. In this way, the apparent viscosity rises to bring about dilatant behavior.

Note that a similar microstructural mechanism, a coil-stretch transition, proved a salient feature of stagnation flows[33]. In particular, it may be responsible for formation of vortices at some stages of the flows. Two kinds of the stagnation flows will be considered in Section 5.

Materials used in polymer flooding. As per [30], synthetic polymers and biopolymers are mostly used in this field, with typical synthetic polymers being *partially hydrolyzed polyacrylamide* (*HPAM*) and its derivatives, and a typical biopolymer being *xanthan gum*. The most of the field projects use HPAM due to its low cost and greater viscoelasticity compared to the xanthan solutions. This work also discusses use of such materials as salinity-tolerant *polyacrylamide* (*KYPAM*), *2-acrylamide-2-methyl propane-sulphonate* (*AMPS*), and *cross-linked polymer gels* in various aspects.

Close the EOL topic by mentioning some limitations of polymeric materials. They may undergo physical and mechanical degradation, perform worse at high salinity and high temperatures[34]. In that regard, wormlike micellar solutions are a perspective alternate to polymers in EOL. Having advantages of viscoelasticity and free from most of the polymers' limitations, they are expected to have edge over polymers[35].

6. On quasi-periodic nature of viscoelastic flows with Newtonian components

Lastly, we will consider some specific traits of benchmark viscoelastic flows, in particular, onset of secondary flows and oscillatory regimes in their dependence on injection of a Newtonian component.

The already cited survey[30], among other aspects of Enhanced Oil Recovery with viscoelastic polymer fluids, discusses the facility problems related to such viscoelastic feature of polymer solutions flows as

development of oscillations. Oscillating stresses cause the pump to vibrate so that, to mitigate the vibration, an increase of the main pipe size is needed. However, viscoelastic behavior of a polymer solution turns out to decrease with an increase of the solvent concentration and *vice versa*.

In this connection, regard now arising of oscillatory vortex-like structures in benchmark flows of viscoelastic mixtures as well as influence of a Newtonian solvent on such flows. Earlier this problem was investigated for the *counterflows in cross slots*[3,4] (**Figure 1**, right part). The rheology was described by the models that proved precise in simulation of benchmark flows. The case of a mono-component fluid was simulated by *upper convected Maxwell* (UCM) constitutive state equation[3,5]. To describe injection of a Newtonian component *Oldroyd-B* model was used. Work[3] suggests "that even minimum viscosity of a Newtonian solvent present in the fluid can 'extinct' (partly or totally) the oscillatory phenomena brought to the mixture by a viscoelastic component".

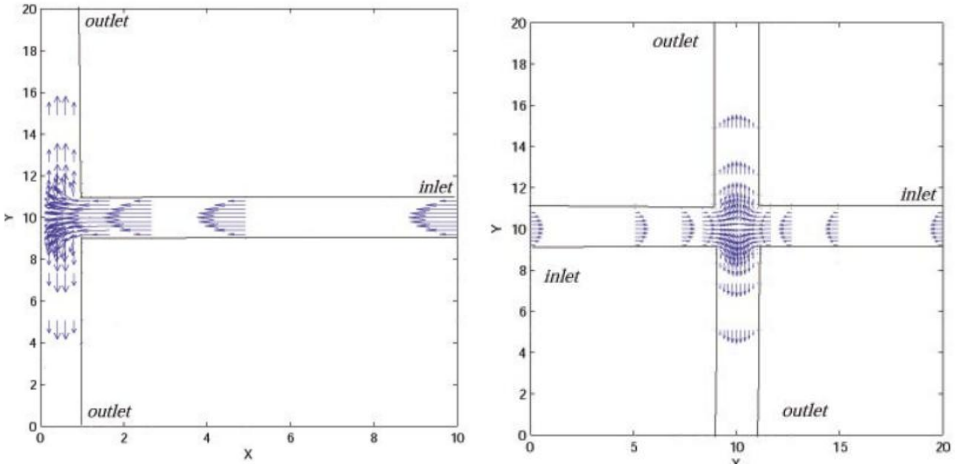

Figure 1; Forms of two benchmark flows of viscoelastic fluid: flow against a wall and counterflows within cross slots**.**

Another benchmark case, a *viscoelastic flow against a wall* (**Figure 1**, left part) was also previously studied for a mono-component fluid meeting the upper convected Maxwell rheological model[4,21]. Present results of this benchmark flow numerical simulation when the fluid is a polymer-solvent mixture.

Problem statement. We thus consider a flow along a horizontal slot (**Figure 1**, left part) reaching the wall of a vertical one to spread over it. In terms of the dimensionless variables normalized on the problem natural scales (asymptotic stationary inlet pressure p_{inlet}, the fluid density ρ, the velocity scale $U=\sqrt{p_{inlet}/\rho}$, and the horizontal slot semi-width d), together with the momentum and continuity equations (here and later, the Einstein notation is used meaning summation on the repeated indices)

$$\frac{\partial v_i}{\partial t}+v_j\frac{\partial v_i}{\partial x_j}=-\frac{\partial p}{\partial x_i}+\frac{\partial \sigma_{ij}}{\partial x_j}, \tag{1}$$

$$\frac{\partial v_i}{\partial x_i}=0, \quad i,j=1,2, \tag{2}$$

we will use two rheological models.

Oldroyd-B model (cf.[3]) describes a mixture of a polymer component (p) and a Newtonian solvent (s) with viscosity

$$\sigma = \sigma^s+\sigma^p. \tag{3}$$

The solvent's viscosity obeys the Newtonian law:

$$\sigma^s_{ij}=\frac{1}{Re_s}\left(\frac{\partial v^i}{\partial x^j}+\frac{\partial v^j}{\partial x^i}\right), \quad i,j=1,2. \tag{4}$$

For the polymer viscosity, we have the Maxwell rheological state equation:

$$\frac{D\sigma^p_{ij}}{Dt}+\frac{1}{De}\sigma^p_{ij}=\frac{1}{Re_p De}\left(\frac{\partial v^i}{\partial x^j}+\frac{\partial v^j}{\partial x^i}\right), \quad i,j=1,2. \tag{5}$$

Here the upper convected Maxwell derivative of the stress tensor is

$$\frac{D\sigma^p_{ij}}{Dt}=\frac{\partial \sigma^p_{ij}}{\partial t}+v_k\frac{\partial \sigma^p_{ij}}{\partial x_k}-\frac{\partial v_i}{\partial x_k}\sigma^p_{kj}-\frac{\partial v_j}{\partial x_k}\sigma^p_{ik}, \quad i,j,k=1,2. \tag{6}$$

The Reynolds numbers for the solvent and polymer components, and the polymer Deborah number are

expressed through the correspondent viscosities and the polymer elastic relaxation time ϑ_p, respectively:

$Re_s = \rho U d / \mu_s$, $Re_p = \rho U d / \mu_p$, $De = \vartheta_p U/d$.

Upper convected Maxwell (UCM) model is actually the Oldroyd-B model applied to a mono-component fluid with: $Re_p \equiv Re$, $\sigma_p \equiv \sigma$, $\sigma_s \equiv 0$

$$\frac{D\sigma_{ij}}{Dt} + \frac{1}{De}\sigma_{ij} = \frac{1}{Re\,De}\left(\frac{\partial v^i}{\partial x^j} + \frac{\partial v^j}{\partial x^i}\right), \quad i, j = 1, 2. \tag{7}$$

As ***initial conditions***, zero values are set for all the dependent variables.

Boundary conditions consist in no-slip constraints at the walls $u_{wall} = v_{wall} = 0$, setting the outlet pressure to 0, and increase of the inlet pressure from 0 up to 1 on the exponential law to reach stationary flow conditions:

$$p_{inlet}(t) = 1 - \exp(-\alpha t).$$

The numerical results below are all obtained for $\alpha = 1$. Varying α did not principally change the results. When $t = \tau \approx 6.5$, then the time derivative of the inlet pressure is less than 0.15% of its initial value. So later on, the flow conditions are considered near-stationary.

System of equations (1)-(7) with the initial and boundary conditions was solved by means of ***the numerical procedure*** described in detail in[4,20]. It is essentially based on *pressure correction method*.

As with the *counterflows*[3,4], it took this flow significantly more time - compared to τ - to get stabilized with moderate and high Deborah numbers. During the stabilization, the spread also involved *flow reversals*. So that the flow resembled a freely oscillating elastic spring. This is illustrated in **Figure 2**: its left and right parts show the flows moving in opposite directions. The middle part presents the change in direction accompanied by a significant decrease of the fluid inlet/outlet volume fluxes, and *arising of large-scale circular structures*. Some residual vortices may persist for certain time after the flow reversal as seen in the figure right part.

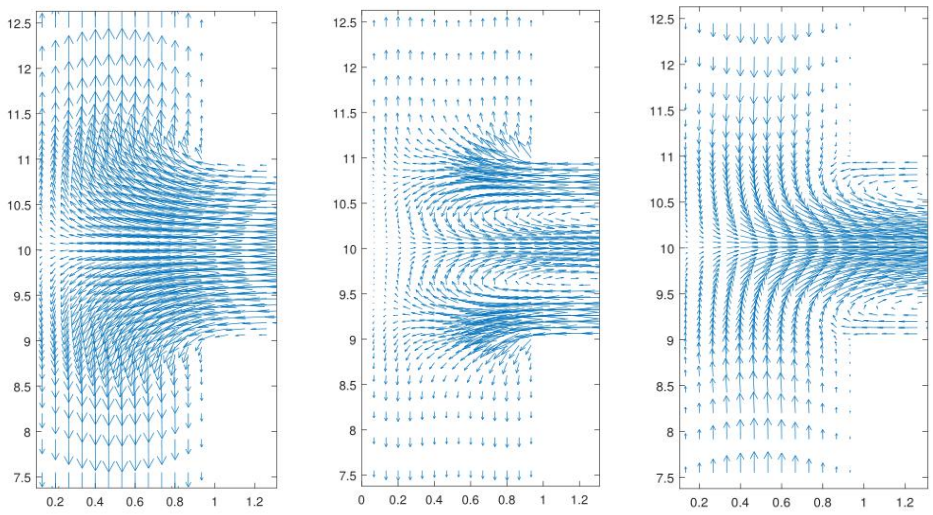

Figure 2; Flow reversal: three snapshots of the Oldroyd-B fluid spreading on the wall**.** $Re_p = 0.1$, $Re_s = 5$, $De = 4$; $t = 1, 1.9, 2.1$**.**

A classical work on computational fluid mechanics[36] suggests using the so-called diagnostic functionals to describe integral characteristics of flows. It proved useful to characterize the degree of the numerical solutions non-stationarity by a functional

$$I(t) = \frac{1}{P}\sum_{i,j}\left(\left|\frac{\partial u_{ij}}{\partial t}\right| + \left|\frac{\partial v_{ij}}{\partial t}\right|\right) \tag{8}$$

expressed through the partial time derivatives of the velocities mesh node values. P is the total number of the nodes. The time dependencies of this functional are shown in **Figure 3** (blue curves for the Oldroyd-B fluid). The figure also shows dependencies of the fluid volume fluxes through the inlet section (magenta curves are for the Oldroyd-B fluid). Evidently, those two kinds of dependencies are closely correlated: at the times of the fluxes' local minima and maxima the flow is mostly stationary and stable, whereas when the fluxes values are somewhere midway between their extrema, the flow reaches the highest degree of non-stationarity. Its structure is most complicated, in particular, because of the circular structures. We can also see that not every fluxes' local maximum brings about a flow reversal. This only happens to the Oldroyd-B fluids with Re_s 5, 10, and 100. With lower Reynolds numbers, or higher viscosities

of the solvent relative to the polymer component ($Re_n / Re_s \le 0.1$), the non-stationarity functional has weak oscillations, and the flux has no oscillations at all. It turns out that still lower relative viscosities of the solvent ($Re_n / Re_s \le 0.02$) result in a non-oscillating flux.

Therefore, injection of a low-viscous Newtonian solvent is able to substantially suppress dynamic elastic features of the flow. This conclusion is close to the situation of another benchmark task, the counterflows within the cross slots, as pointed out above.

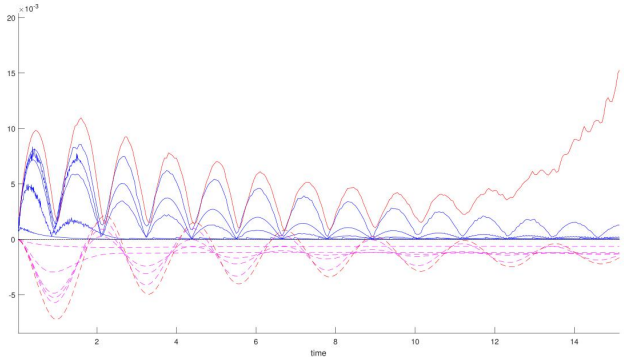

Figure 3; Time dependencies of the non-stationarity functional (8) (solid lines) and inlet fluid volume fluxes (dashed lines). The blue solid lines (in ascending order) and magenta dashed lines (in descending order) correspond to Oldroyd-B fluids with *De*=4, Re_p=0.1, and Re_s respectively, 0.1, 1, 5, 10, 100. The red (top and bottom) lines are pertinent to the UCM fluid with *De*=4, *Re*=0.1**.**

The conclusion is also close to the statement from[28]. This book, in particular, presents a quasi-periodic behavior of a viscoelastic fluid Poiseuille flow in terms of UCM and Oldroyd-B models and refers to a number of experimental works with direct observations of these phenomena. It suggests: "Even a small Newtonian viscosity component can considerably diminish the resonance amplitude, especially for small tube radii, which is interpreted as the result of viscous damping".

We will state, therefore, that significant suppression of viscoelastic oscillatory behavior by a small portion of a Newtonian solvent can be thought of as a universal trait of viscoelasticity. Evidently, this may be of practical interest in the technological processes where stability and regularity of flows are important.

Peculiarities of the UCM fluid flow. As seen in **Figure 3**, all the five curves of the non-stationarity functional (8) for the Oldroyd-B fluid tend to zero, which means that the flows reach a stationary state after establishing stationary flow conditions. However, this is not the case of the upper curve corresponding to the UCM fluid. Tending to get stabilized at the beginning, later on (at *t* >12) the UCM fluid flow becomes less and less stationary.

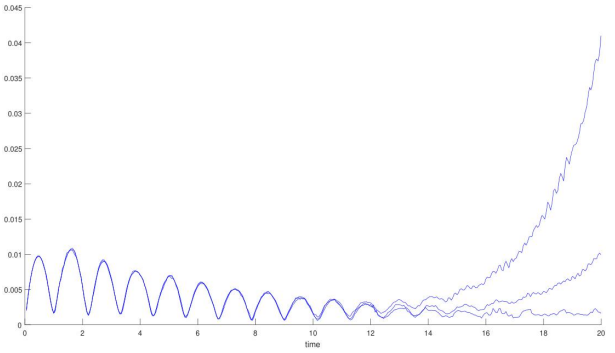

Figure 4; Time dependencies of the non-stationarity functional (8) for the UCM fluid flow with *De*=4, *Re*=0.1. The calculations are performed on mashes of different fineness: 900, 1296, 1600 nodes in order of the curves increase**.**

This curve is also shown in **Figure 4** together with two more curves obtained with the domain partitions of other fineness. Therefore, the rate of non-stationarity rise depends significantly on the computational procedure. **Figure 5** shows the flow field in the vicinity of the stagnation point at the wall, the region of high strains. It contains a number of small-scale vortex-like structures. Further calculation, up to *t*=30, resulted in a burst of instability.

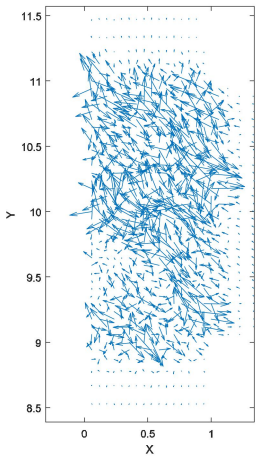

Figure 5; Vicinity of the stagnation point of very non-stationary UCM fluid flow. *De*=4, *Re*=0.1, *t*=20. The computational mesh is 1600 nodes**.**

Presently it is hard to figure out whether this is a natural or computational instability. In fact, it might be a loss of computational solution depending on numerical configuration because three curves related to three different domain partitions look differently. Much more mesh sizes were actually tried, and they also gave different rates of non-stationarity functional increase (or no increase at all).

However, all the curves almost coincide up to some point ($t \approx 12$). Later on, the curves still look smooth enough. In that regard, there is a possibility that the difference in the curves rise might be due to emergence of small-scale vortices. The finer the mesh, the more precisely they can be apparently described by the numerical solution to make the curve grow more intensively. If there emerges a cascade of vortices with different scales, the observed behavior may indicate development of elastic turbulence[37]. This sophisticated point is worth further detailed investigation.

7. Conclusion

In this manner, by considering five important subjects of modern rheology we try to extend the point formulated at the beginning: phenomena encountered in complex fluids flows are often mutually connected and governed by common laws of viscoelastisity. The variety of the traits involved is underlain by the variety of the scales a complex fluid elastic constituents have. The scales range between the molecular and the flow levels. In this, the variety of relationships between *elastic* and *viscous* factors is material-specific.

As a result, we can observe shear bands when the flow curve of a viscoelastic material is non-monotonic.

Specific manifestation of viscoelasticity in zones of high strain formed by obstacles, stagnation points or in porous media gives rise to anomalies and instabilities in such zones. Due to finite relaxation times in the fluid, these zones often spread downstream, and interact with one another.

When a special form of the flow domain dictates non-stationary restructuring of the whole of the flow (the case of capillaries), to account for elastic forces very precise knowledge of relaxation times – their spectrum – is needed.

In various experimental and industrial situations, manifestation of viscoelasticity essentially depends on the presence of a Newtonian solvent. The ability of solvents to effectively “extinct” viscoelastic traits seems to be their universal hallmark.

The main point of this work can therefore be formulated as follows: good understanding of viscoelasticity fundamental nature is a key to understanding of a large variety of polymeric and other complex fluids behavior. It also provides means to control many industrial processes.

References

1. Divoux T., Fardin M., Manneville S., *et al.* Shear banding of complex fluids. Annual Review of Fluid Mechanics 2016; 48: 81-103.
2. Siginer D. Quasi-Periodic Flows of Viscoelastic Fluids in Straight Tubes. In Developments in the Flow of Complex Fluids in Tubes. Springer International Publishing, 2015. 65-78.
3. Mackarov I. Numerical observation of transient phase of viscoelastic fluid counterflows. Rheologica acta 2012; 51(3): 279-287.
4. Mackarov I. Viscoelastic flows with a stagnation point: regularity, instability, bifurcations. ISBN 978-620-2-00327-8. LAMBERT Academic Publishing, 2017.
5. Mackarov I. Asymmetries and bifurcations of viscoelastic counterflows in cross slots. Fluid Dynamics Research 2014; 46(4): 041413.
6. Fielding S. Linear instability of planar shear banded flow. Physical review letters 2005; 95(13): 134501.
7. Milner S., McLeish C., Likhtman A. Microscopic theory of convective constraint release. Journal of Rheology 2001; 45(2): 539-563.
8. Olmsted P. Perspectives on shear banding in complex fluids. Rheologica Acta 2008; 47(3): 283-300.
9. Chaudhuri P., Berthier L., Bocquet L. Inhomogeneous shear flows in soft jammed materials with tunable attractive forces. Physical Review E 2012; 85(2): 021503.
10. Salipante P., Little C., Hudson S. Jetting of a shear banding fluid in rectangular ducts. 2017; Physical review fluids 2(3): 033302.
11. Dhont J., Kang, K., Lettinga, M., *et al.* Shear-banding instabilities. Korea-Australia Rheology Journal 2010; 22(4): 291-308.
12. Fielding S. Linear instability of planar shear banded flow. Physical review letters 2005; 95(13): 134501.
13. Mackarov I. Dynamic features of viscoelastic fluid counter flows. Annual Transactions of the Nordic Rheology Society 2011; 19: 71-79.
14. Sarkar A., Donald L. A model for complex flows of soft glassy materials with application to flows through fixed fiber beds. Journal of Rheology 2015; 59(6): 1487-1505.

15. Gibaud T., Barentin C., Taberlet N., *et al*. Shear-induced fragmentation of laponite suspensions. Soft Matter 2009; 5(16): 3026-3037.
16. Wapperom P., Renardy M. Numerical prediction of the boundary layers in the flow around a cylinder using a fixed velocity field. Journal of Non-Newtonian Fluid Mechanics 2005; 125: 35-48.
17. Haward S., Sharma V., Odell J. Extensional opto-rheometry with biofluids and ultra-dilute polymer solutions. Soft Matter 2011; 7(21): 9908-9921.
18. Haward S. Buckling instabilities in dilute polymer solution elastic strands. Rheologica acta 2010; 49(11-12): 1219-1225.
19. Varshney A., Steinberg V. Drag enhancement and drag reduction in viscoelastic flow. arXiv preprint 2018; arXiv:1809.03778.
20. Mackarov I. Is a UCM fluid flow near a stationary point always singular? arXiv preprint 2016; arXiv:1602.02404.
21. Mackarov I. Is a UCM fluid flow near a stationary point always singular?-Part II. arXiv preprint 2016; arXiv:1606.07980.
22. Rodriguez F., Cohen C., Ober C., *et al*. Principles of polymer systems (6th ed.). CRC Press, 2014.
23. Agassant J., Avenas P., Carreau P., *et al*. Polymer processing: principles and modeling (2nd ed.).. Carl Hanser Verlag GmbH Co KG, 2017. 39
24. Malkin A., Ilyin S., Vasilyev G., *et al*. Pressure losses in flow of viscoelastic polymeric fluids through short channels. Journal of Rheology 2014; 58(2): 433-448.
25. McDougall I., Orbey N., Dealy J. Inferring meaningful relaxation spectra from experimental data. Journal of Rheology 2014; 58(3): 779-797.
26. Evangelista S., Leopardi A., Pignatelli R., *et al*. Hydraulic transients in viscoelastic branched pipelines. Journal of Hydraulic Engineering 2015; 141(8): 04015016.
27. Meniconi S., Brunone B., Ferrante M. Water-hammer pressure waves interaction at cross-section changes in series in viscoelastic pipes. Journal of fluids and structures 2012; 33: 44-58.
28. Siginer D. Developments in the Flow of Complex Fluids in Tubes. Springer International Publishing, 2015. 57, 71-76.
29. Malkin A., Zuev K., Arinina M., *et al*. Modifying the viscosity of crude heavy oil by using surfactants and polymer additives. Energy & Fuels 2018.
30. Sheng J., Leonhardt B., Azri N. Status of Polymer-Flooding Technology. Journal of Canadian Petroleum Technology 2015; 54(02): 116-126.
31. Urbissinova T., Trivedi J., Kuru E. Effect of Elasticity during Viscoelastic Polymer Flooding-A Possible Mechanism of Increasing the Sweep Efficiency. In SPE western regional meeting. Society of Petroleum Engineers 2010.
32. Pathak J., Ross D., Migler K. Elastic flow instability, curved streamlines, and mixing in microfluidic flows. Physics of Fluids 2004; 16(11): 4028-4034.
33. Carrington S., Odell J. How do polymers stretch in stagnation point extensional flow-fields? Journal of Non-Newtonian Fluid Mechanics 1996; 67: 269-283.
34. Zhong H., Zhang W., Fu J., *et al*. The performance of polymer flooding in heterogeneous type II reservoirs—An experimental and field investigation. Energies 2017; 10(4): 454.
35. Kumar S., Awang M., Abbas G., *et al*. Wormlike Micellar Solution: Alternate of Polymeric Mobility Control Agent for Chemical EOR. Journal of Applied Sciences 2014; 14: 1023-1029.
36. Williams G. Numerical integration of the three-dimensional Navier-Stokes equations for incompressible flow. Journal of Fluid Mechanics 1969; 37(4), 727-750.
37. Fouxon A., Lebedev V. Spectra of turbulence in dilute polymer solutions. Physics of Fluids 2003; 15(7): 2060-2072.